Spectral Data Fusion for Robust ECG-derived Respiration with Experiments in Different Physical Activity Levels

Iman Alikhani[1], Kai Noponen[1], Arto Hautala[1], Rahel Ammann[2] and Tapio Seppänen[1]
[1]*Physiological Signal Analysis Group, Center for Machine Vision and Signal Analysis, University of Oulu, Oulu, Finland*
[2]*Swiss Federal Institute of Sport, Magglingen, Switzerland*
{*iman.alikhani, kai.noponen, arto.hautala, tapio.seppanen*}*@oulu.fi, rahel.ammann@baspo.admin.ch*

Keywords: Respiratory Sinus Arrhythmia, Heart Rate Variability, Spectral Fusion, R-peak Amplitude, QRS Morphological Shape, Time-frequency Analysis, Robustness, Single-channel ECG.

Abstract: In this paper, we study instant respiratory frequency extraction using single-channel electrocardiography (ECG) during mobile conditions such as high intensity exercise or household activities. Although there are a variety of ECG-derived respiration (EDR) methods available in the literature, their performance during such activities is not very well-studied. We propose a technique to boost the robustness and reliability of widely used and computationally efficient EDR methods, aiming to qualify them for ambulatory and daily monitoring. We fuse two independent sources of respiratory information available in ECG signal, including respiratory sinus arrhythmia (RSA) and morphological change of ECG time series, to enhance the accuracy and reliability of instant breathing rate estimation during ambulatory measurements. Our experimental results show that the fusion method outperforms individual methods in four different protocols, including household and sport activities.

1 INTRODUCTION

Respiratory frequency is a vital physiological signal used for a variety of diagnostic and clinical purposes. Often, it is not measured just by itself but together with other vital signals using a multitude of sensors to judge correlations between a patient's physiology and different diseases. Especially in ambulatory monitoring, where the measurements are made during regular daily activities, the sensors, however, might interfere with and change the breathing rhythms of subjects and cause discomfort. Since instantaneous breathing rate can be estimated indirectly using ECG signal, development of ECG-derived respiration (EDR) software tools could decrease the cost and facilitate making long-term measurements in a more pleasant and true-to-life manner.

The concept of EDR was proposed decades ago in (Moody et al., 1985) and clinically validated in (Moody et al., 1986). Basically, the estimation of EDR is enabled by two physiological phenomena:

- The heart rate (HR) is modulated by the respiration such that R-R intervals (RRI) shorten during inhale and elongate during exhale, which is known as the respiratory sinus arrhythmia (RSA).
- The mechanical effects of chest movement during breathing modulates the observed ECG morphology, which is especially visible in the QRS-complex part and can be measured, e.g. as either R-peak amplitude (RPA) or the morphological scale variation of QRS complexes (MSV).

These derived quantities – RRI, RPA and MSV – are employed widely in published EDR methods that operate on single-channel ECG (Cysarz et al., 2008; Thayer et al., 2002; Schäfer and Kratky, 2008; Correa et al., 2008; Orphanidou et al., 2013; Noponen et al., 2012). A proportion of publications contributing in EDR area, attempt to extract the respiratory time series waveform (Correa et al., 2008; Cysarz et al., 2008; Widjaja et al., 2012), while, some other studies, including our own paper, focus on acquiring breathing rate of subjects regardless of the respiratory waveform morphology (Schäfer and Kratky, 2008; Thayer et al., 2002; Orphanidou et al., 2013).

In 2008, the three following comparison papers were published in the EDR area. The first paper (Schäfer and Kratky, 2008) studied various EDR methods based on RSA and proposed a time-domain counting method to estimate instantaneous respiratory frequency. In the second paper (Correa et al., 2008), the authors compared breathing morphology derived from RRI, RPA and area under R wave (AUR) sig-

Alikhani, I., Noponen, K., Hautala, A., Ammann, R. and Seppänen, T.
Spectral Data Fusion for Robust ECG-derived Respiration with Experiments in Different Physical Activity Levels.
DOI: 10.5220/0006144100880095
In *Proceedings of the 10th International Joint Conference on Biomedical Engineering Systems and Technologies (BIOSTEC 2017) - Volume 5: HEALTHINF*, pages 88-95
ISBN: 978-989-758-213-4

nals with the reference breathing phase recorded from both plethysmography and nasal air flow signals. The third paper (Cysarz et al., 2008), compares the performance of the estimated breathing rate derived from RPA and RRI signal with the actual values and experimented on a database consisting of sleep and wake data. The first paper claims that spectral-based EDR estimation cannot produce accurate results and time-domain advanced counting method is a more stable alternative for the EDR problem which could offer higher correlation. The second paper, concludes that the correlation coefficient between AUR based EDR and plethysmography signal is 0.56 after temporal delay matching, making AUR superior to both the RPA and the RSA by more than 0.05. One limitation of the study is the small data set that they have experimented with. The authors of the third paper found fairly decent agreement (concordance correlation coefficient of 0.41 to 0.79 within different age groups) between the EDR estimation and reference respiration. They also noted that RSA components strength weaken for people over 50 years old which is in agreement with the findings of the first paper.

Although fairly good correspondence has been achieved with rather inactive subjects, morphological variation of ECG that is generated by respiration-related chest movement can be contaminated by a person's movement, body position changes, and upper/lower limb motions; especially during sport activities. Consequently, there is a clear need for a robust EDR method that can tolerate such interference and remain reliable.

The aforementioned EDR methods estimate the respiration from the ECG derived quantities rather directly. More advanced techniques have been proposed in search for a more dependable EDR method to be able to assess breathing frequency or rhythm more robustly. Decomposition-based EDR methods, including principal component analysis (PCA) and kernel PCA, were investigated in (Widjaja et al., 2012). In addition, adapted PCA and independent component analysis (ICA) were utilized in (Tiinanen et al., 2009; Tiinanen et al., 2015) to extract the RSA component from RRI signal and subsequently estimate the breathing rate of subjects. Recently, a robust technique was published in (Orphanidou et al., 2013), which they proposed a selective framework that evaluates both RPA and RRI signals selecting the one with more strongly modulated respiratory component. They represented the filtered RPA and RRI signals with auto regressive (AR) models. An AR model considers the signal to be characterized by a number of spectral poles. They picked the pole within the respiratory band with higher magnitude as the estimated breathing frequency. This model assumes that pole magnitude is a metric for the signal quality and apparently higher quality signal contains distinctive respiratory fluctuation. They claimed that this selective framework outperforms EDR estimations compared to individual RPA and RRI signal by 0.5 and 0.02 unit of mean absolute error (MAE), respectively, in young subjects and 0.14 and 0.13 unit within elderly subjects.

In order to address EDR throughout sport activities, it should be noted that apart from potential artifacts during such measurements, physiological cardiolocomotion coupling (CLC) component is introduced in the heart activity. It is already reported that there is a coupling between locomotor, respiration and heart (Nomura et al., 2003). CLC is caused by the cadence of running, walking or activities which involves limb movement and exterior impacts from floor coming toward body. The rhythmic cadence of subjects alters HRV signal in a periodic manner, by influencing muscle pump on the circulatory system and cardiac reflexes (Novak et al., 2007). This makes EDR estimation an even more challenging problem during mobile activities, particularly at higher exercise intensities.

Although EDR is an old-standing topic in physiological signal analysis, the performance of methods during typical daily activities, specifically household and sport activities, is not very well-examined in the literature. Our goal in this paper is to evaluate widely-used EDR techniques and propose a preliminary robust framework for instant breathing rate estimation throughout uncontrolled ambulatory condition where a mobile subject performs daily activities. We analyze the signals in a robust way to extract the most correlated component to the instant respiratory frequency. To this extent, we are using a fusion technique to make the system redundant, in case artifact, CLC or any other components alter the extracted instantaneous respiratory estimation.

2 MATERIALS AND METHODS

In this section, the construction of signals expected to contain respiratory frequency information is explained. The modeling of signal's spectral content using AR time-frequency model and their adjustments, as well as the fusion of information acquired by individual sources are described.

2.1 Calculation of RRI, RPA and MSV

Single-channel ECG is recorded concurrently with a spirometer signal. In the subsequent ECG processing, there are some steps that are followed before extraction of RRI, RPA and MSV signals.

Firstly, baseline wander reduction has been performed using a second-order Savitzky-Golay filter with one second window. The filter fits a polynomial function with the given order on each frame of ECG data minimizing the least-squares error, and replaces the considered sample with the fitted value. We assume that the fitted function follows the baseline of the ECG signal closely. Therefore, we subtract the baseline from the ECG.

Secondly, the R-peaks of the ECG are detected. We passed the signal through a 20th-order high-pass Butterworth IIR filter using a zero-phase digital filtering technique to suppress P and T waves and keep R waves steady. The output of filter is explored (using MATLAB findpeaks function) for peaks with specific criteria, including passing a minimum amplitude, minimum peak prominence and peak separation. Applied constraints filter the detected local maximas to R-peaks.

Thirdly, the results of R-peak detection are used in the calculation of derived quantities. The RRI signal is obtained from the successive R-peak time stamp differences as RR_i, where the ith value of this signal is equal to the difference of ith and $i+1$th time stamp of R-peaks. However, the detection of some ectopic beats or false beats is likely when the subjects are performing exercise and daily activities freely. To counteract this, ectopic/false beat detection and editing is conducted using the following procedure:

1. Detect and reject the obvious outliers ($RR_i \leq 200$ ms or $RR_i \geq 2000$ ms). Such intervals are rare in a healthy subject's heart rhythm due to physiological considerations.
2. Estimate short term RRI level by fitting a smoothing spline function on the signal, and consider the absolute difference between the actual RRI values and the smoothed one as an indicator on how much the RRI deviates from the local level.
3. Detect ectopic/false beats as those with RR_is with large deviation from the short term RRI level. More precisely, mark the ones which deviate both more than 50 ms and also more than $95th$ percentile of all deviations from the spline.
4. Interpolate over ectopic/false and outlier beats with spline interpolation, to preserve the number of beats of the initial detection.

Using the aforementioned procedure, it is assured that less than 5% of the RR_is are edited. Accordingly, the RPA signal can be constructed from the ECG amplitudes at R-peak instants. The construction of MSV is explained comprehensively in (Noponen et al., 2012). Initially, a 50 ms window is defined symmetrically around detected R-peak locations. It is followed by the collection of all QRS complexes within the window in a matrix and a definition of a statistical mean shape as a template for the scale variation measure. The candidate QRS complexes are projected into the template and the scale difference between them is considered as MSV signal.
Finally, we use an 8 Hz spline interpolation to have uniformly sampled signal in further spectral analysis. A sample of ECG segment as well as constructed and interpolated signals are depicted in Figure 1.

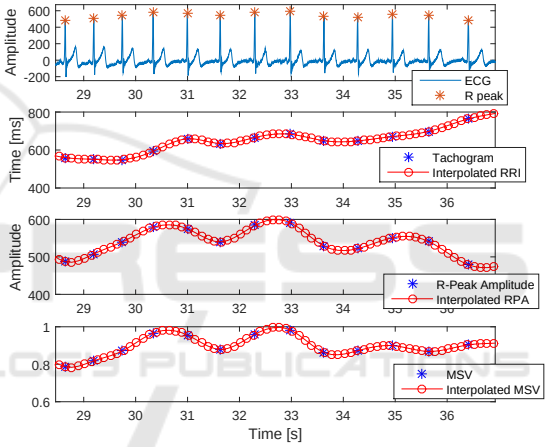

Figure 1: A segment of ECG with constructed signals. Top most sub-figure shows the ECG segment in blue and R-peak annotations are expressed by red stars. The second sub-figure shows original RRI samples. RPA signal is depicted in the third sub-figure and MSV time series in the fourth sub-figure. In the last three sub-figures, the interpolated samples are marked in red, and original values in blue.

2.2 Spectral Analysis

We are aiming to extract instant breathing frequency from the constructed signals. Usually, breathing rate of a healthy subject in normal condition varies roughly between 10 to 36 breaths per minute (bpm), while in our application where the subjects are exercising or performing activities, the breathing rate might be over 60 bpm. Therefore, we use a relatively wide band-pass filter with low and high cut-off frequencies of 0.15 Hz and 1.2 Hz corresponding to 9 bpm and 72 bpm. Figure 2 shows the frequency response of the band-pass filter.

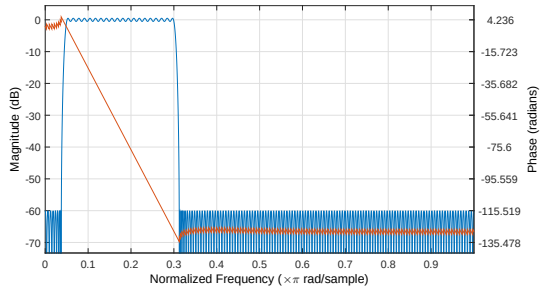

Figure 2: The magnitude and phase response of the FIR filter used to keep the spectral content of signals within the possible respiratory frequency. 60 dB and 1 dB is adjusted as the stop- and pass-band attenuation. Sampling frequency is 8 Hz and the x-axis is the normalized frequency.

2.2.1 AR Model

Physiological signals are principally non-stationary, which requires specific tools for spectral analysis. In this study, according to (Thayer et al., 2002; Orphanidou et al., 2013) recommendation, we have used 12th-order AR model on 20-second segments of data which has 19 seconds overlap with adjacent windows. This model considers an all-pole transfer function to describe the frequency distribution of signal. The higher the order of AR model, the more poles are used for the signal description. A sample AR model outcome is illustrated in Figure 3.

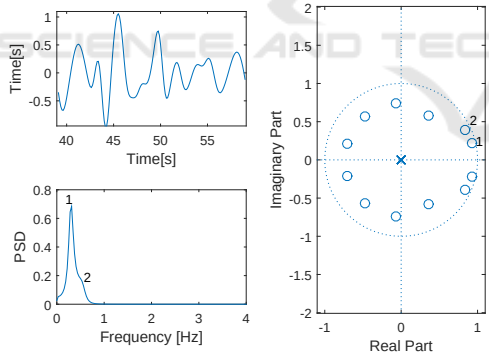

Figure 3: A 20-second segment of interpolated and filtered RRI signal is fed to the AR model and output zero-pole plot is depicted in the right unity circle. Lower left sub-figure illustrates the power spectral density (PSD) of the upper left RRI time series. The local trends of the PSD labeled by 1 and 2 are constructed as a result of poles labeled by 1 and 2 in the z-plane. These two poles are higher in magnitude and closer to unity circle which means they have stronger effect on the construction of PSD curve.

To derive the respiratory frequency from the spectrum, in the case of a single source EDR using RRI, RPA or MSV, we find the frequency bin having highest power spectral density. For instance in the lower left sub-figure of Figure 3, the frequency value of signal marked as 1 is considered as the respiratory frequency for this segment of data.

2.3 Fusion of PSDs

According to the EDR literature, the power spectra of RRI, RPA and MSV signals within a short time window are expected to contain energy at or near the instantaneous respiratory frequency. In addition, the respiratory component is expected to usually be strong in the sense that spectral power levels around the respiratory frequency are higher than the background levels in each spectrum. However, the spectra are expected to also contain other peaks rising from noise/artifacts, CLC, nonlinearities, and also side lobes induced by amplitude and/or frequency modulation by physiological feedback loops such as the control of heart rate through RSA, for instance.

Due to the different nature of RRI, RPA, and MSV, it can be assumed that the strength of the aforementioned other factors varies between their spectra, but the respiration component should be present in all or most of them. Thus, it makes sense to attempt to find significant energy bands or peaks that are present in all of the spectra. What is more, even when the respiratory component is present in all of them, the redundant combination can be used to narrow down the actual respiratory frequency as the resolving power of individual spectra depends on the width/peakedness of the spectral peak that can vary.

In this paper, we approach the issue via spectral domain fusion that strengthens the joint spectral components and diminishes the ones not shared with other spectra. We hypothesize that the fusion will be advantageous in instantaneous breathing rate estimation. Let's assume that the spectrogram of constructed signals can be expressed as:

$$P_{sig} = \begin{pmatrix} p^{sig}_{1,1} & p^{sig}_{1,2} & \cdots & p^{sig}_{1,n} \\ p^{sig}_{2,1} & p^{sig}_{2,2} & \cdots & p^{sig}_{2,n} \\ \vdots & \vdots & \ddots & \vdots \\ p^{sig}_{m,1} & p^{sig}_{m,2} & \cdots & p^{sig}_{m,n} \end{pmatrix} \quad (1)$$

where *sig* could be RRI, RPA or MSV signal. Every column in the spectrogram corresponds to the PSD of signal in a specific 20-second time window which has one second difference with the consecutive columns of matrix and every row, to the lied energy at specific frequency band. In the fusion matrix, we compute the product of these arrays element-by-element. It should be noted that these PSDs contain the same number of values. Thus, the fusion spectrogram can be stated as:

$$P_{fus} = \begin{pmatrix} p^{rri}_{1,1} \cdot p^{rpa}_{1,1} \cdot p^{msv}_{1,1} & p^{rri}_{1,2} \cdot p^{rpa}_{1,2} \cdot p^{msv}_{1,2} & \cdots & p^{rri}_{1,n} \cdot p^{rpa}_{1,n} \cdot p^{msv}_{1,n} \\ p^{rri}_{2,1} \cdot p^{rpa}_{2,1} \cdot p^{msv}_{2,1} & p^{rri}_{2,2} \cdot p^{rpa}_{2,2} \cdot p^{msv}_{2,2} & \cdots & p^{rri}_{2,n} \cdot p^{rpa}_{2,n} \cdot p^{msv}_{2,n} \\ \vdots & \vdots & \ddots & \vdots \\ p^{rri}_{m,1} \cdot p^{rpa}_{m,1} \cdot p^{msv}_{m,1} & p^{rri}_{m,2} \cdot p^{rpa}_{m,2} \cdot p^{msv}_{m,2} & \cdots & p^{rri}_{m,n} \cdot p^{rpa}_{m,n} \cdot p^{msv}_{m,n} \end{pmatrix} \quad (2)$$

P_{fus} basically gives a joint spectrogram which considers the agreement between individual spectrogram trends as well as their strength. The frequency bin where the maximum energy is settled at each time instant, is selected as the estimated respiratory frequency. In case there is a correlation between at least two of the signal's PSDs with sufficient strength, the fusion PSD also offers the same trend in the fusion spectrum. However, if there is no correlation between PSDs, the fusion spectrum is affected by the PSD with higher energy. In other words, the fusion method intuitively considers the signal with stronger component as suggested in (Orphanidou et al., 2013) and also decides in a cooperative manner.

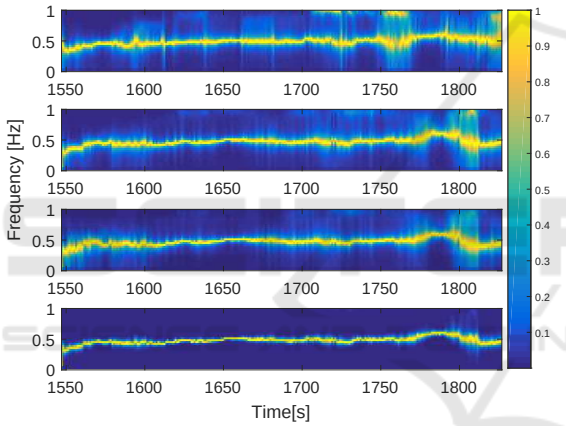

Figure 4: A sample 100-second spectrogram of the constructed signals plus the fusion spectrogram. All the spectrograms are normalized at each time instant for better visualization. The top most sub-figure illustrates RRI, the second top is RPA and the third row shows the MSV normalized spectrogram and the bottom sub-figure is the normalized fusion spectrogram.

It is conceivable that in specific cases and time instants other combinations of spectrograms – such as the joint product of a certain pair of them – may yield better performance than the product triplet. Nevertheless, we expect the presented approach, in which the element-wise multiplication is taken over all the three spectrograms, to perform better on average. Thus, in the following, we consider only the fusion (2) that combines RRI, RPA, and MSV spectrograms.

In Figure 4, the normalized spectrograms of a sample RRI, RPA and MSV signals taken at the same time are depicted. The normalized fusion spectrogram is illustrated in the last sub-figure. Wide distribution of energy in some parts of individual spectrograms is visible, while the fusion spectrogram (bottom sub-figure) earns the common component between the individual spectrums and is considerably narrower.

2.4 Database

Since, in this study, we are aiming to evaluate the performance of our instantaneous respiratory frequency estimation methods during uncontrolled ambulatory measurements where the subjects can freely perform their daily activities, we have collected 67 subjects (30 female and 37 male) aged from 18 to 60 years old during household and sport activities. The overall general physiological characteristics of subjects are stated in Table 1.

Table 1: General characteristics of subjects participated in this experiment.

Characteristic	mean	min	max
Height (cm)	175	160	195
Weight (Kg)	75.4	45.6	122.8
Age ($Years$)	37.9	18	60
BMI (Kg/m^2)	24.51	14.72	35.5

The ECG signal is recorded using an available commercial electrode belt in the market and upsampled to 1 kHz for HRV analysis and the spirometer data is collected at the rate of one sample per second.

The household activities are comprised of four minutes of floor sweeping (FS) followed by four minutes of table cleaning (TC). The sports activity part of the protocol consists of 10 minutes of cycling (CY) on an ergometer, followed by four minutes of Tennis playing (TN) in a gym hall. During these activities, both spirometer and single-channel ECG data are collected. The relative intensity level of four activity protocols is given in Table 2 as the overall percentage of maximal heart rate (HR_{max}) of subjects in that specific activity.

Table 2: Overall intensity of activity protocols as a percentage of HR_{max}.

Activity Protocol	mean	min	max
FS	52	35	73
TC	50	34	77
CY	66	48	83
TN	81	63	90

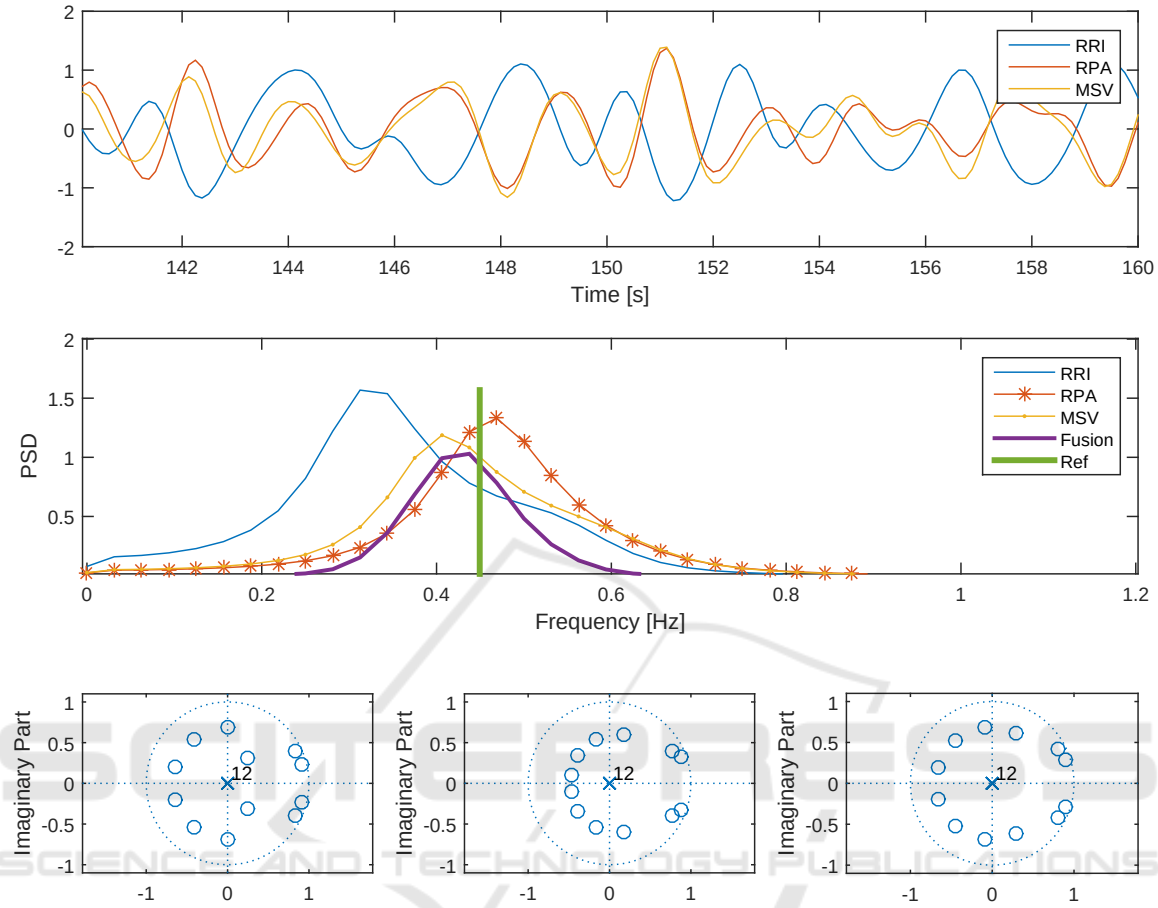

Figure 5: A 20-second sample household activity data including interpolated and filtered RRI, RPA and MSV signal as well as their PSD in the middle sub-figure. The last sub-figure shows RRI, RPA and MSV *z*-plane, respectively, from left to right.

3 RESULTS

3.1 Performance Measures

Let's assume that our estimated breathing frequency is expressed as x and the original respiratory frequency as y and n is the number of samples, in order to assess our estimation results, the following metrics are computed:

- Root Mean Square Error:

$$RMSE = \sqrt{\frac{1}{n}\sum_{j=1}^{n}(x_j - y_j)^2} \tag{3}$$

- Mean Absolute Percentage Error: MAPE weights frequency of respiration. Basically, it considers a larger error margin in higher breathing rate estimation.

$$MAPE = \frac{1}{n}\sum_{j=1}^{n}\left|\frac{x_j - y_j}{y_j}\right| \tag{4}$$

- Concordance Correlation Coefficient: It is a reliable measure to evaluate the agreement between two sets of signals. It can be computed using

$$R_c = \frac{2S_{xy}}{S_x^2 + S_y^2 + (\hat{y} - \hat{x})^2} \tag{5}$$

where $\hat{x}$ and $\hat{y}$ are the average frequency of estimated and original signals and

$$S_{xy} = \frac{1}{n}\sum_{j=1}^{n}(x_j - \hat{x})(y_j - \hat{y}) \tag{6}$$

and S_x and S_y are the standard deviation of x and y, respectively.

3.2 Quantitative Results

Figure 5 illustrates a 20-second sample data. It shows the signals, their frequency components distributions and specification of poles. In the middle sub-figure, three PSDs as well as computed fusion PSD are depicted. Reference respiratory frequency is also expressed by a straight green line. Instant breathing rate estimation using PSD is corresponded to the frequency where maximum energy is settled.

Table 3 summarizes the results of the methods used in four activity protocols. The data shows that the fusion method outperforms the individual methods in all the four protocols considering different metrics. The performance of EDR derived from RRI signal (RSA-based breathing frequency estimation) is the weakest compared to other two individual signals particularly in sport activities. It might be due to the reason that RRI signal is more vulnerable to CLC or movement artifacts during high intensity exercise.

Table 3: Acquired overall results in four different activity protocols.

Spect	Metric	Activity			
		FS	TC	CY	TN
RRI	RMSE	6.2	5.4	5.3	8.3
	MAPE	19.0	18.0	16.0	18.0
	Rc	0.23	0.19	0.39	0.33
RPA	RMSE	5.0	4.5	3.4	6.9
	MAPE	16.0	15.0	10.0	15.0
	Rc	0.2	0.18	0.57	0.39
MSV	RMSE	4.7	4.4	3.7	6.4
	MAPE	15.0	14.0	11.0	13.0
	Rc	0.25	0.19	0.5	0.43
Fusion	RMSE	4.6	4.1	2.9	6.4
	MAPE	14.0	13.0	8.8	13.0
	Rc	0.28	0.24	0.57	0.45

4 CONCLUSION

Ambulatory measurement of instantaneous respiratory frequency can be achieved via ECG surrogate signal processing. However, the performance of breathing rate estimation during uncontrolled condition when the subject is free to move and perform his/her daily activities is in question and not well-studied. This paper proposed a spectral fusion technique which combines the information from individual sources of EDRs, such as RSA-based (RRI signal) and morphological-based (RPA and MSV signals), to boost the performance of estimation using computationally-efficient methods. In essence, the presented method considers the agreement between the individual estimators and their joint spectral power. Overall, our fusion method outperforms the individual methods considering all the metrics and experimented activity protocols.

REFERENCES

Correa, L. S., Laciar, E., Torres, A., and Jane, R. (2008). Performance evaluation of three methods for respiratory signal estimation from the electrocardiogram. In *2008 30th Annual International Conference of the IEEE Engineering in Medicine and Biology Society*, pages 4760–4763. IEEE.

Cysarz, D., Zerm, R., Bettermann, H., Frühwirth, M., Moser, M., and Kröz, M. (2008). Comparison of respiratory rates derived from heart rate variability, ecg amplitude, and nasal/oral airflow. *Annals of biomedical engineering*, 36(12):2085–2094.

Moody, G. B., Mark, R. G., Bump, M. A., Weinstein, J. S., Berman, A. D., Mietus, J. E., and Goldberger, A. L. (1986). Clinical validation of the ecg-derived respiration (edr) technique. *Group*, 1(3).

Moody, G. B., Mark, R. G., Zoccola, A., and Mantero, S. (1985). Derivation of respiratory signals from multi-lead ecgs. *Computers in cardiology*, 12(1985):113–116.

Nomura, K., Takei, Y., and Yanagida, Y. (2003). Comparison of cardio-locomotor synchronization during running and cycling. *European journal of applied physiology*, 89(3-4):221–229.

Noponen, K., Tiinanen, S., and Seppänen, T. (2012). Deriving respiration from the electrocardiogram by serial comparison with statistical mean shape. In *2012 Computing in Cardiology*, pages 809–812. IEEE.

Novak, V., Hu, K., Vyas, M., and Lipsitz, L. A. (2007). Cardiolocomotor coupling in young and elderly people. *The Journals of Gerontology Series A: Biological Sciences and Medical Sciences*, 62(1):86–92.

Orphanidou, C., Fleming, S., Shah, S. A., and Tarassenko, L. (2013). Data fusion for estimating respiratory rate from a single-lead ecg. *Biomedical Signal Processing and Control*, 8(1):98–105.

Schäfer, A. and Kratky, K. W. (2008). Estimation of breathing rate from respiratory sinus arrhythmia: comparison of various methods. *Annals of Biomedical Engineering*, 36(3):476–485.

Thayer, J. F., Sollers III, J. J., Ruiz-Padial, E., and Vila, J. (2002). Estimating respiratory frequency from autoregressive spectral analysis of heart period. *IEEE Engineering in Medicine and Biology*, 21(4):41–45.

Tiinanen, S., Noponen, K., Tulppo, M., Kiviniemi, A., and Seppänen, T. (2015). Ecg-derived respiration methods: Adapted ica and pca. *Medical engineering & physics*, 37(5):512–517.

Tiinanen, S., Tulppo, M., and Seppänen, T. (2009). Rsa component extraction from heart rate signal by independent component analysis. In *2009 36th Annual Computers in Cardiology Conference (CinC)*, pages 161–164. IEEE.

Widjaja, D., Varon, C., Dorado, A., Suykens, J. A., and Van Huffel, S. (2012). Application of kernel principal component analysis for single-lead-ecg-derived respiration. *IEEE Transactions on Biomedical Engineering*, 59(4):1169–1176.